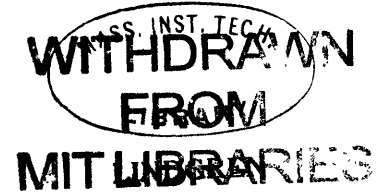




THE REFINEMENT OF THE STRUCTURE  
OF SULVANITE,  $\text{Cu}_3\text{VS}_4$

by

Felix John Trojer  
Dr. phil., University of Graz  
(1964)



SUBMITTED IN PARTIAL FULFILLMENT  
OF THE REQUIREMENTS FOR THE  
DEGREE OF MASTER OF  
SCIENCE

at the

MASSACHUSETTS INSTITUTE OF TECHNOLOGY

June, 1966

Signature of Author

\_\_\_\_\_  
Department of Geology, May 20, 1966

Certified by

Thesis Supervisor *J* \_\_\_\_\_

Accepted by

\_\_\_\_\_  
Chairman, Departmental Committee  
on Graduate Students

# Refinement of the structure of sylvanite

by

Felix J. Trojer

Submitted to the Department of Geology on  
May 20, 1966 in partial fulfillment of the requirements  
for the degree of Master of Science.

## Abstract

The structure of sylvanite,  $\text{Cu}_3\text{VS}_4$  was solved by Pauling and Hultgren (1933). The bonding of V to S is an unusual one which, it was thought, warranted checking and refining the structure. The crystals have symmetry  $\overline{P}43m$  with  $a = 5.3912 \pm 0.0007 \text{ \AA}$ .

A set of intensity data was collected with an equi-inclination diffractometer using Zr-filtered  $\text{MoK}\alpha$  radiation. During the course of the refinement it became necessary to correct observed intensities which showed a contribution from white radiation streaks of other reflections of smaller  $\theta$ . With this corrected set of data the unweighted  $R$  dropped to 9.8% and the weighted  $R$  to 5.2%.

The refinement confirmed Pauling and Hultgren's structure proposal for sylvanite. The improved value of the positional parameter of S is  $x = 0.2372 \pm 0.0003$ , which leads to a V - S distance of  $2.214 \pm 0.0009 \text{ \AA}$  and Cu - S distance of  $2.297 \pm 0.001 \text{ \AA}$ . An electron-density difference map suggested that the sulfur atom cannot be represented by a spherical electron-density distribution modified by an elliptical thermal motion. The V atom has a very sharp peak and a small temperature factor whereas the Cu peak indicated a considerable anisotropic thermal motion.

The appendix lists two computer programs, MINTE 1 and MINTE 2, which were devised and used to correct observed intensities which are affected by white-radiation streaks.

Thesis supervisor: Martin J. Buerger

Title: Professor of Mineralogy and Crystallography

Table of contents

	<u>Page</u>
Abstract . . . . .	2
List of figures . . . . .	4
List of tables . . . . .	5
Introduction . . . . .	6
Data collection . . . . .	7
Unit cell and space group . . . . .	7
Alignment of the diffractometer . . . . .	7
Counter and pulse-height-analyser settings . . . . .	8
Intensity measurements and corrections . . . . .	10
Confirmation of Pauling and Hultgren's structure proposal. . .	14
White radiation streak correction . . . . .	17
Refinement . . . . .	22
Discussion of the structure . . . . .	31
Appendix . . . . .	36
MINTE 1 . . . . .	36
MINTE 2 . . . . .	42
Acknowledgements . . . . .	47
References . . . . .	48

List of figures

	<u>Page</u>
Figure 1. Horizontal and vertical distribution of intensity across the pinhole system . . . . .	9
Figure 2. Counter-voltage plateau . . . . .	11
Figure 3. Intensity distribution . . . . .	12
Figure 4. Schematic Patterson map, Sections $\underline{P}(0yz)$ , (a) Sphalerite type. (b) Sulvanite type. . . . .	15
Figure 5. Plot of $\underline{R}_\lambda$ versus $\lambda$ . . . . .	19
Figure 6. Variation of the $\underline{R}$ value in respect to $\underline{F}_{obs}$ . . . . .	26
Figure 7. Electron-density difference map for sulvanite. (a) Orientation of the sections in respect to the unit cell. (b) Section along (110). (c) Section parallel to (111) on which the copper peaks from the density map are projected. . . . .	34

List of tables

	<u>Page</u>
Table 1. Original atomic parameters, L. Pauling and R. Hultgren (1933). . . . .	16
Table 2. Comparison of h00 and hh0 reflections before and after the streak correction . . . . .	21
Table 3. Computation of restrictions on the $\beta_{ij}$ . . . . .	25
Table 4. Final $\underline{F}_{obs}$ and $\underline{F}_{calc}$ of sulvanite. . . . .	27
Table 5. Final positional parameters and isotropic temperature factors of sulvanite. . . . .	32
Table 6. Interatomic distances in sulvanite. . . . .	32
Table 7. Bond angles between atoms in sulvanite. . . . .	33
Table 8. Anisotropic temperature coefficients for the atoms in sulvanite. . . . .	33

### Introduction

The crystal structure of sylvanite was first investigated by W. F. deJong (1928) by means of powder photographs. His structure was based upon a cubic cell with  $a = 10.772 \text{ \AA}$  and containing eight  $\text{Cu}_3\text{VS}_4$ . Later Pauling and Hultgren (1933) pointed out that the experimental data published by deJong did not necessarily lead to such a large cell edge. With Laue and oscillation photographs, they found that  $a = 5.386 \text{ \AA}$  and the cell contains only one formula unit of  $\text{Cu}_3\text{VS}_4$ . Laue photographs along the main crystal axes and the body diagonal showing four-fold and three-fold symmetry respectively. This limited the possible space groups to  $\underline{\text{P}\bar{4}3\text{m}}$ ,  $\underline{\text{P}432}$ ,  $\underline{\text{P}4/\text{m}\bar{3}2/\text{m}}$ . By comparing the even-order reflection with the calculated structure factors, Pauling and Hultgren eliminated two space groups, leaving  $\underline{\text{P}\bar{4}3\text{m}}$  as the only possible one for sylvanite.

### Data collection

Unit cell and space group. The experimental work reported here was done with a specimen from Mercur, Utah, from the Harvard Museum collection, kindly loaned by Professor Clifford Frondel. A spectroscopic analysis of these sulvanite crystals, provided by Mr. William Blackburn of the Cabot Spectroscopic Laboratory, MIT, showed the absence of any substitution for V by other metals such as As and Sb. W. F. deJong (1928) found in the early investigation that his crystals were also very close to the ideal composition  $\text{Cu}_3\text{VS}_4$ .

An accurate value of the cell edge was determined from a back-reflection Weissenberg photograph using  $\text{CuK}\alpha$  radiation. The result,  $a = 5.3912 \pm 0.0007 \text{ \AA}$ , is consistent with the values  $5.390 \text{ \AA}$  found by Lundquist and Westgren (1936) and  $5.391 \text{ \AA}$ , given by L. G. Berry and R. M. Thompson (1962). The space group,  $\text{P}\bar{4}3\text{m}$ , determined from Friedel symmetry of the precession photographs and the tetrahedral habit, is the same as reported by L. Pauling and R. Hultgren (1933).

Alignment of the diffractometer. A rectangular crystal having dimensions  $0.21 \times 0.11 \times 0.06 \text{ mm}$  was selected for intensity measurements. Precise adjustments on the diffractometer were necessary to assure that the whole crystal was within the cross section of constant intensity of the x-ray beam.

The procedure of this alignment is as follows: A small aperture is moved across the x-ray beam between the counter and the collimator to sample the intensity distribution in horizontal and vertical direction. For this purpose it is convenient to use a flat piece of lead with a very narrow hole, for instance  $0.03 \times 0.08 \text{ mm}$ , mounted on a goniometer head. This device is aligned on the diffractometer in the same manner as a crystal so that the small hole can be seen through the pinhole system.

By turning the spindle of the crystal-rotating assembly, the narrow hole is moved left and right. By plotting intensity versus translation the horizontal intensity distribution across the collimator opening can be examined. In order to record the amount of translation on the dial, an indicator is attached to the spindle. The first scan usually shows an asymmetric profile, suggesting that the settings of the leveling screws of the diffractometer base be adjusted. This changes the position of the whole diffractometer and therefore also of the pinhole system in respect to the fixed direction of the x-ray beam coming out through the tube window. After a few attempts the recording shows a symmetric plateau having a sufficient width to include the whole crystal. (Compare Fig. 1.)

After adjusting the horizontal cross section, the vertical one has to be examined in a similar way. To translate the aperture up and down, the vertical sledge of the goniometer head has to be moved by turning the little spindle of the sledge with a special wrench on which there has been attached a dial for determining the amount of translation. In the same manner as before, a profile is obtained, and again a suitable plateau can be achieved by adjusting the leveling screws of the base. The plot in Fig. 1 combines these results, and shows two perpendicular scans across the collimator opening. They indicate that the plateau of constant intensity is more than large enough to cover the longest dimension of the crystal. It is worth checking the cross section of the x-ray beam again after the data collection to assure that the cross section has remained unchanged.

Counter and pulse-height analyser settings. To maintain the same amplification of signals from a scintillation detector throughout the whole data collection, a suitable counter voltage has to be selected. To do this the detector voltage is slowly varied from lower to higher



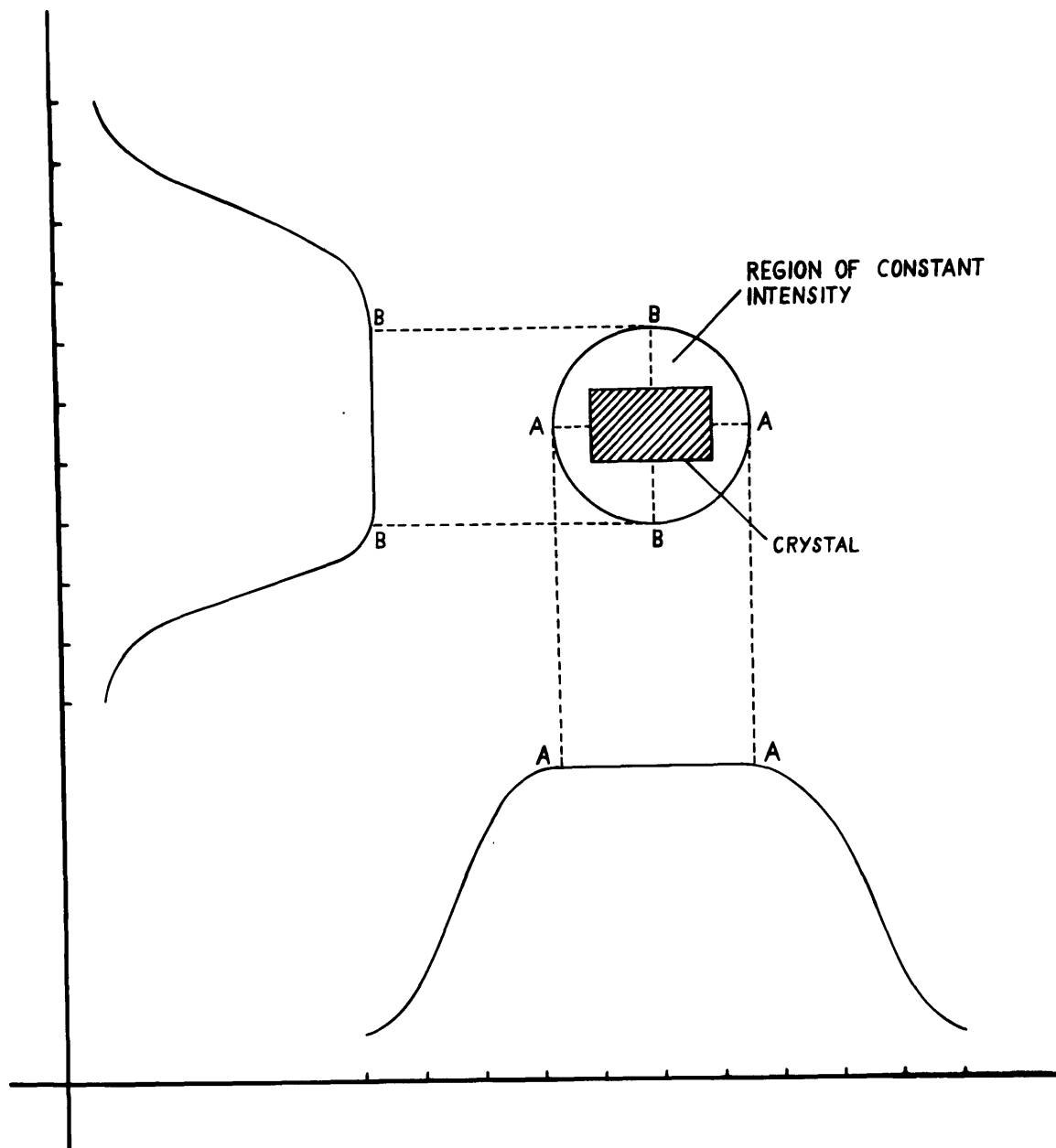


Fig. 1 Horizontal and vertical distribution of intensity across the pinhole system.

values, while the intensity from a strong crystalline reflection is examined using integral recording and a low base level, for instance 5 V. When this is done a graph like Fig. 2 is obtained, showing that, if 760 V is selected as the proper voltage, small variations of this setting during the operation time would not result in a detectable change of amplification. The base line or base level is a variable discriminator threshold setting, which allows pulses to be cut off below a certain desired energy level (this is described in the Norelco Radiation Detectors Instruction Manual). In order to count x-ray quanta with a scintillation detector within a given energy range, and to reject quanta of greater and lesser energy, the pulse-height analyser of the electronic circuit panel has to be adjusted, (see Norelco Radiation Detectors Instruction Manual). The energy range to be used is determined by the width of the intensity distribution of the x-ray quanta. This distribution, of which a differential recording is shown in Fig. 3, was obtained using a 2 V energy range, and lowering the discriminator threshold from high to low voltage with the automatic motor drive. An appropriate energy range, of 23 V referred to as the window width, was obtained from the intensity distribution shown in Fig. 3. From the same graph the lower boundary of this window, namely the discriminator threshold or base line, was found to be 11 V. With these settings all intensities will result from pulses which have an energy within the base line and base line plus window width. At the same time care was taken not to exceed the linearity range of the scintillation detector. This was effected by using absorbers if the number of counts per second was more than 10000.

Intensity measurements and corrections. About 300 reflections were collected by means of an equi-inclination diffractometer using Zr-filtered MoK $\alpha$  radiation. This was operated manually.

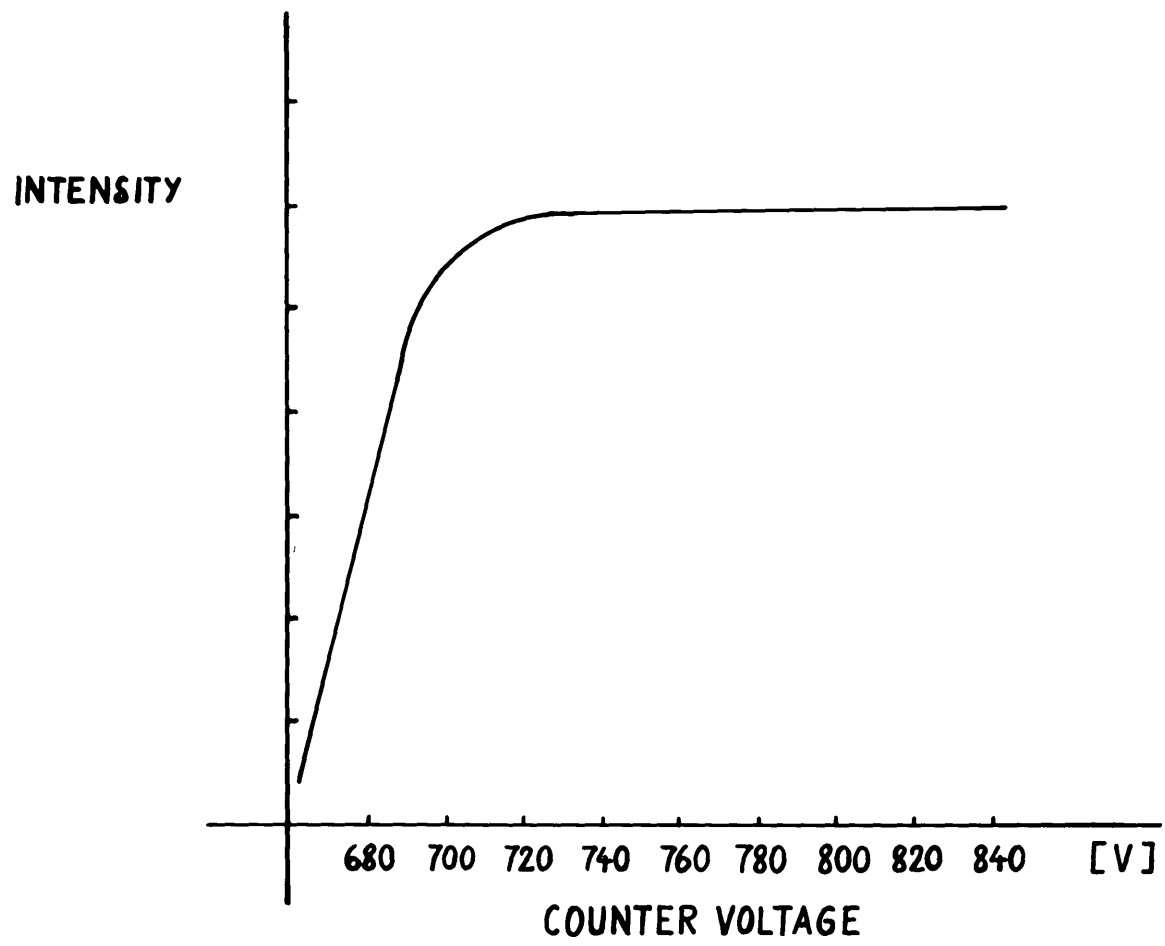


Fig. 2 Counter-voltage plateau.

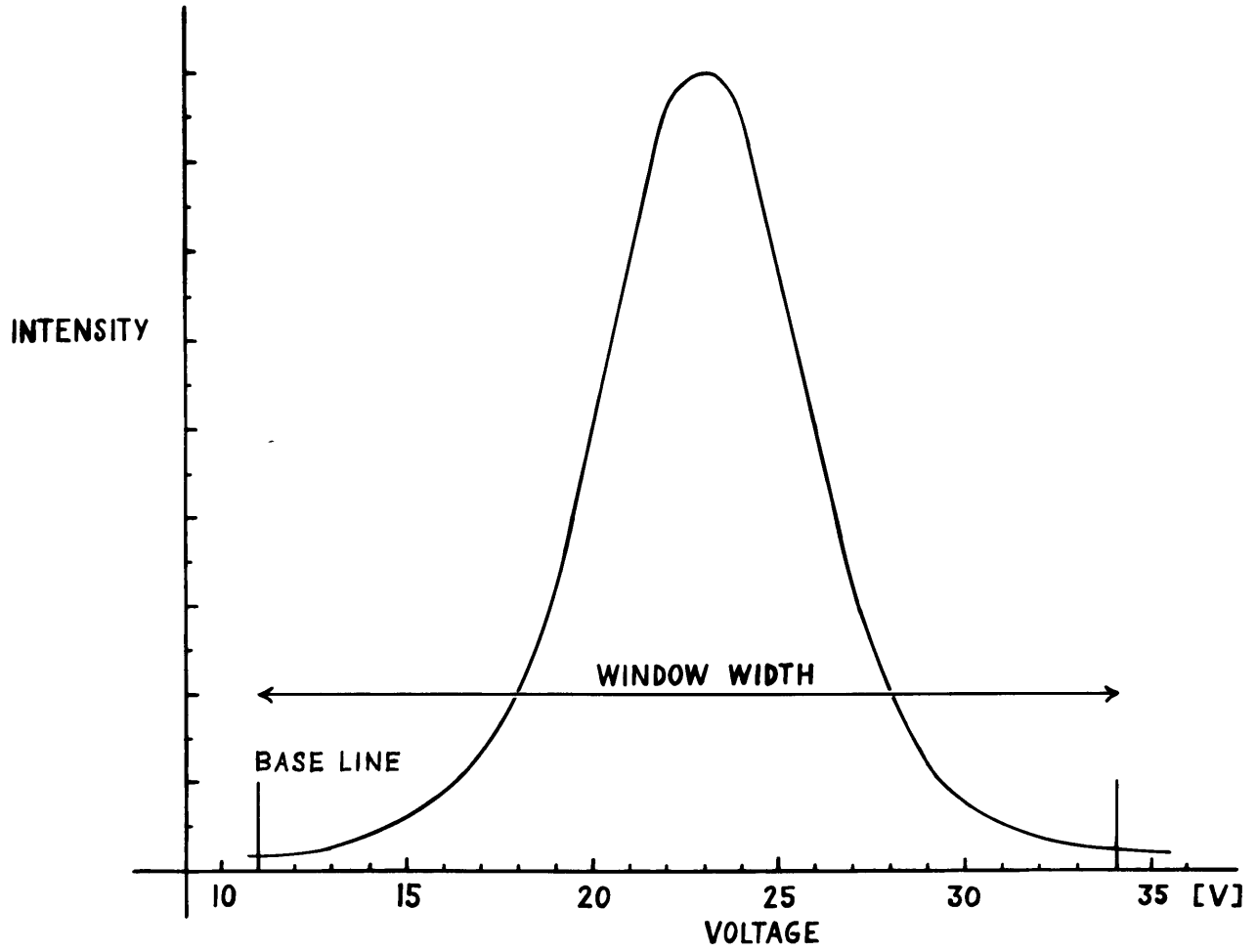


Fig. 3 Intensity distribution.

Despite the small size of the crystal, the difference in the transmission factors between the shortest and longest path of the x-ray beam through the crystal was about 10%. Accordingly the measured intensities were corrected for absorption as well as Lorentz and polarization factors using the IBM 7094 program GAMP, written by H. H. Onken (1964), and GNABS, written by C. W. Burnham, see H. H. Onken (1964).

### Confirmation of Pauling and Hultgren's structure proposal.

A three dimensional Patterson map, of which a schematic section at  $\underline{x} = 0$  is shown in Fig. 4, indicated that a sphalerite-type structure is not possible for sulvanite. This conclusion had been reached by Pauling and Hultgren through intensity comparison on Laue photographs.

A preliminary set of structure factors was calculated with the coordinates found by Pauling and Hultgren, listed in Table 1. The signs from this set of  $\underline{F}_{\text{cal}}$  were attributed to  $\underline{F}_{\text{obs}}$ , and with these Fourier coefficients a three-dimensional electron-density map was computed using the IBM 7094 program MIFR 2 written by D. P. Shoemaker (1965, unpublished). With a preliminary scale factor and isotropic temperature factors, the discrepancy factor  $\underline{R}$ , was 18.3%. The  $\underline{R}$  value and an electron-density map were sufficient to show that the structure obtained by Pauling and Hultgren was substantially correct.

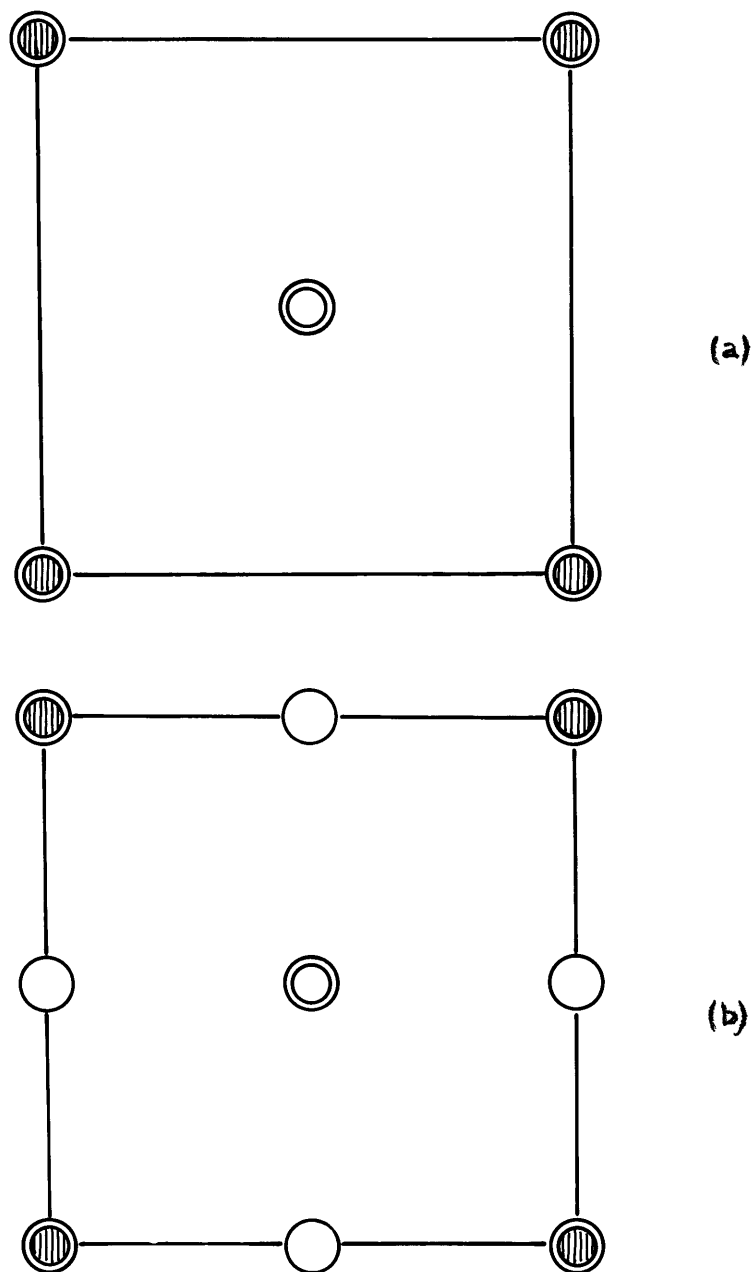


**Fig. 4** Schematic Patterson map, sections  $\underline{P}$  ( $0yz$ )

(a) Sphalerite type. (b) Sulvanite type. The single circle represents the peak due to V-Cu, the double circle the peaks due to Cu-Cu, and S-S, and the partly filled circle the peaks due to V-V, Cu-Cu, and S-S.

Table 1

Original atomic parameters of L. Pauling and R. Hultgren (1933)

Atom	Equipoint	Symmetry	$\underline{x}$	$\underline{y}$	$\underline{z}$
V	$\underline{1a}$	$\overline{43m}$	0	0	0
Cu	$\underline{3d}$	$\overline{42m}$	$\frac{1}{2}$	0	0
S	$\underline{4e}$	$\underline{3m}$	0.235	0.235	0.235



White-radiation streak correction

A comparison of zero-level Weissenberg photographs obtained with  $\text{CuK}\alpha$  and  $\text{MoK}\alpha$  radiation revealed that the latter had a strong polychromatic component. For this reason some reflections were actually located on white-radiation streaks corresponding to other reflections located on the same lattice line. Hence some reflections collected with the diffractometer using  $\text{MoK}\alpha$  radiation had abnormally high intensities, as compared with the same reflections recorded on a Weissenberg picture with  $\text{CuK}\alpha$  radiation.

Using an equi-inclination diffractometer it is, in general, not possible to distinguish a peak superimposed on a white radiation streak from a peak without such a contribution. In fortunate cases the different shape and the flat top identifies a scan through a lattice point affected by a radiation streak. In order to correct these affected reflections it is necessary to know the intensity distribution along a lattice line. This matter was discussed by A. C. Larson (1965). The desired intensity distribution can be found by using a lattice line with a strong reflection at the lowest possible  $\theta$ ; this reflection cannot be affected by other radiation streaks. Starting with this small  $\theta$  value, the intensities along the lattice line are measured up to a sufficiently large  $\theta$  value, where the contribution from the first strong peak is negligible. These data are to be corrected for change in effective window width, Lorentz and polarization factor, and processed applying the following equation:

$$R_{\lambda} = I_{\lambda} / I_{\lambda}(\text{K}\alpha)$$

Where  $R_{\lambda}$  is the ratio of the intensity  $I_{\lambda}$ , which is measured along the radiation streak, to  $I_{\lambda}(\text{K}\alpha)$ , which is the true intensity of the  $\lambda(\text{K}\alpha)$  peak

from the first strong reflection.

Since  $\underline{I}_{\lambda(K\alpha)}$  cannot be measured with a normal counter width, it is necessary to evaluate its true magnitude by calibrating the streak correction on known intensities. This can be done easily if the crystal has reflections with about zero intensity along this lattice row, or if the space-group symmetry gives rise to extinctions. In this manner a scale factor  $\underline{S}$  is determined, and the equation above is changed to:

$$R_{\lambda} = \underline{I}_{\lambda} / \underline{I}_{\lambda(K\alpha)} \cdot \underline{S}$$

For this purpose the lattice line  $hh0$  was examined. On this line, 220 was a very strong reflection and 330 had an intensity close to zero. The scale factor  $\underline{S}$  turned out to be equal to 2.2. A plot of  $\underline{R}_{\lambda}$  versus wave length for Mo radiation showed that, when using a Zr filter, substantial intensity due to the polychromatic component occurs in a range of wave length from  $\lambda = 0.6 \text{ \AA}$  up to  $\lambda = 1.2 \text{ \AA}$ , (see Fig. 5). Assuming a reflection with the indices  $\underline{nh} \underline{nk} \underline{nl} = \underline{nH}$  having a white radiation contribution from other reflections  $\underline{iH}$ , where  $\underline{i} < \underline{n}$ , the proper wave length causing this contribution can be calculated applying the Bragg equation in the following form:

$$\lambda_i = 2d_{iH} \sin \theta_{nH}$$

From the plot in Fig. 5,  $\underline{R}_{\lambda}$  is obtained, and the observed intensity  $\underline{I}_{\underline{nH}}$  can be corrected using the equation (A. C. Larson, 1965):

$$\text{corrected } \underline{I}_{\underline{nH}} = \underline{I}_{\underline{nH}} - \sum_{i=a}^{\underline{n}-1} \underline{I}_{iH} \cdot \underline{R}_{\lambda_i} \cos \theta_{nH} \quad n > a,$$

where  $\underline{I}_{iH}$  is the  $\underline{i}$  th intensity affecting  $\underline{I}_{\underline{nH}}$  by its white-radiation streak.  $\underline{R}_{\lambda_i}$  is defined as the percentage of  $\underline{I}_{iH}$  contributing to  $\underline{I}_{\underline{nH}}$ . Since the

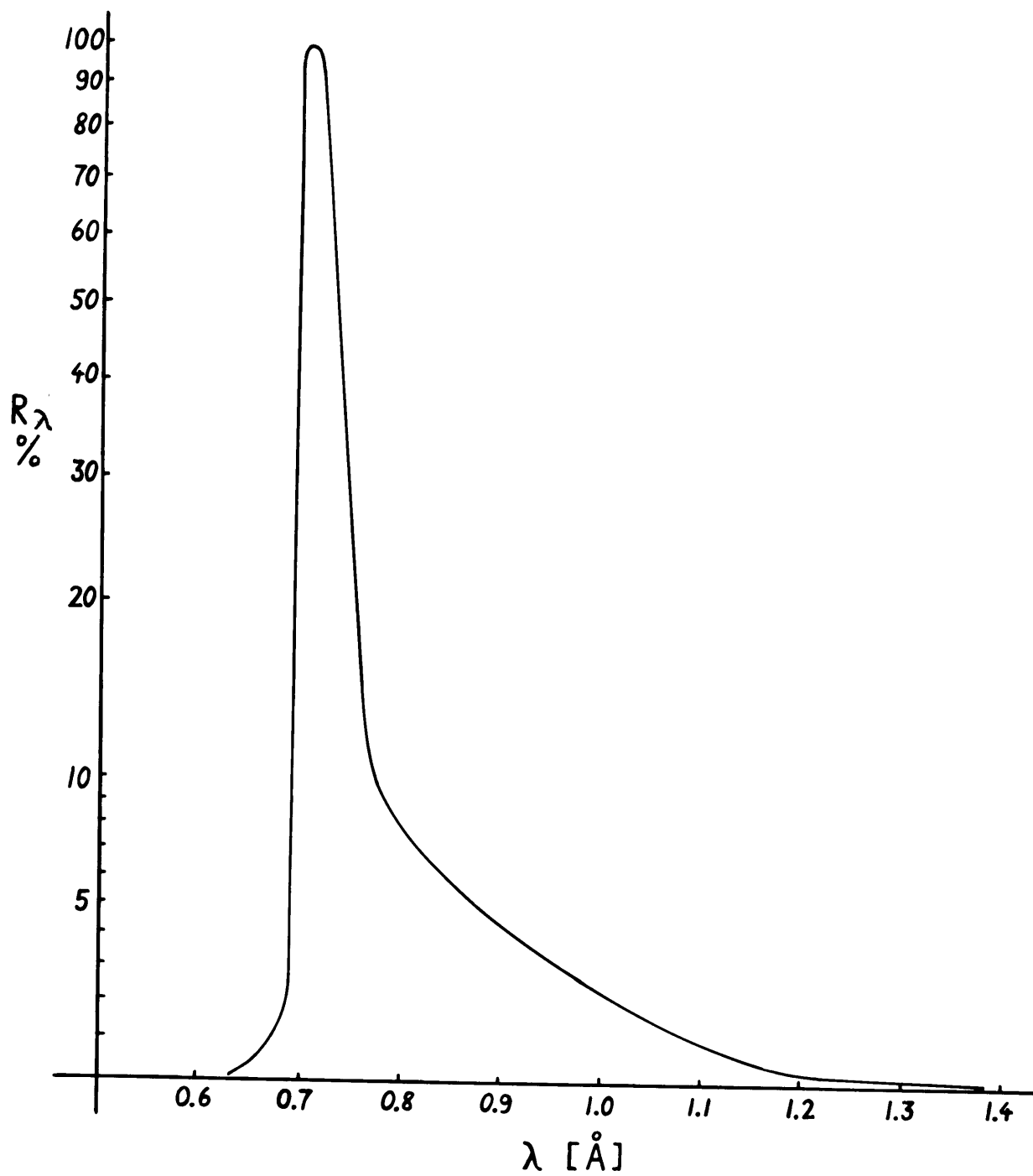


Fig. 5 Plot of  $R_\lambda$  versus  $\lambda$ .

range of wavelength seen through a counter window is dependant on  $\theta$ , a correction term has to be applied to the value of  $I_{iH}$ . It was found that  $\cos \theta_{nH}$  is a good approximation for the change of the effective window width. A. C. Larson, 1965, uses  $\csc \theta$ .

A reinvestigation of the observed intensities of sulvanite showed that, out of 287 reflections which were used in this refinement, 39 of them included a considerable contribution from the white radiation of other reflections of smaller  $\theta$ . In order to correct these effected intensities, two IBM 7094 programs, MINTE 1 and MINTE 2, were written (see Appendix).

Table 2, which lists reflections along the lattice lines h00 and hh0, before and after the correction, shows an improved agreement between  $F_{obs}$  and  $F_{calc}$ . Similar results were obtained with all the other reflections which were significantly affected.

Table 2

Comparison of h00 and hh0 reflections before and after the streak correction.

h	k	l	with correction		without correction	
			F <sub>obs</sub>	F <sub>calc</sub>	F <sub>obs</sub>	F <sub>calc</sub>
2	0	0	83.66	78.23	83.66	78.22
3	0	0	47.38	44.13	48.31	43.94
4	0	0	153.59	152.02	153.83	151.97
5	0	0	57.20	52.02	65.92	52.05
6	0	0	34.11	29.28	36.86	29.34
7	0	0	10.89	5.64	14.12	5.41
8	0	0	58.43	54.28	58.51	54.24
9	0	0	27.40	23.81	35.20	23.77
10	0	0	13.50	14.08	17.59	14.12
11	0	0	5.93	1.34	8.16	1.16
12	0	0	18.59	17.66	18.69	17.62
13	0	0	5.85	8.99	5.85	8.90
14	0	0	7.04	7.18	7.04	7.18
3	3	0	2.47	2.19	23.18	2.10
4	4	0	99.33	101.46	99.33	101.45
5	5	0	1.73	5.59	21.14	5.72
6	6	0	50.06	48.06	50.06	48.09
7	7	0	2.31	7.13	11.78	7.21
8	8	0	22.26	22.08	22.26	22.13
9	9	0	7.70	5.43	9.54	5.44
10	10	0	8.81	10.01	8.81	10.03

### Refinement

A least-squares refinement of this corrected set of data was carried out with the SFLSQ 3 program written by C. T. Prewitt and recorded by H. H. Onken (1964). Due to experimental errors some observed structure factors are more likely to be in error than others. In order to decrease the influence of the more inaccurate data on the least-square refinement, several weighting schemes have been proposed (A. deVries, 1965). Following deVries' suggestion, this structure was first refined as well as possible with an arbitrary weighting scheme (in this case equal weights for all reflections) and then a weighting scheme based on the discrepancy between  $\underline{F}_{\text{obs}}$  and  $\underline{F}_{\text{calc}}$  was used. The application of the latter scheme can be justified on the ground that, at this stage of the refinement it was apparent that the essential features of the structure of sulvanite were correct. Accordingly a statistical comparison between  $\underline{F}_{\text{obs}}$  and  $\underline{F}_{\text{calc}}$  was made by calculating residuals  $\underline{R} = \sum ||\underline{F}_{\text{obs}}| - |\underline{F}_{\text{calc}}|| / \sum |\underline{F}_{\text{obs}}|$  for groups of 20 reflections. These  $\underline{R}$  values, representing the probable errors in the observed structure factors, were plotted versus each of the corresponding averages over 20  $\underline{F}_{\text{obs}}$ , as shown in Fig. 6. A suitable weighting scheme was obtained, based on the inverse of this curve, by assigning equal weights to reflections with  $|\underline{F}_{\text{obs}}| > 30$ , and different weights to reflections with  $|\underline{F}_{\text{obs}}| < 30$ , namely  $\underline{w} = \underline{F}_{\text{obs}} / \underline{k}$  in which  $\underline{k} = 40$ .

Several cycles of refinement, allowing all parameters to vary, yielded to an unweighted  $\underline{R}$  value of 10.6% and a weighted  $\underline{R}$  of 5.8%. Since a difference synthesis suggested that the Cu atoms had considerable anisotropic thermal motion, an attempt was made to represent each atom by four fractional atoms (Kantha and F. R. Ahmed, 1960). It was

thought that the copper atom performs an anharmonic vibration towards interstices not occupied by sulfur atoms. A similar case was observed by B. T. M. Willis (1965) in fluorite. The point-group symmetry  $\bar{4}2m$  of the Cu site allowed four fractions of the atom to be displaced symmetrically in the four tetrahedral directions pointing to the adjacent holes at  $x\bar{x}\bar{x}$ ,  $\bar{x}xx$ ,  $x\bar{x}x$ , and  $\bar{x}\bar{x}\bar{x}$ , where  $x$  is the positional parameter of the S atom. Assuming a displacement of 0.005 Å, the new coordinates of the Cu atom in fractions of the cell edge were 0.501, 0.001, 0.001. Two cycles of refinement led to an unweighted  $\underline{R}$  of 10.6% and weighted  $\underline{R}$  of 5.7%. Since no significant improvement of the residual resulted, and the isotropic temperature factor of the Cu atom even showed a slight increase, no further trials were performed.

Up to the present stage of refinement the scattering factors of neutral Cu, V, and S were used in the calculation of the structure factors. Various possible valencies for Cu, V, and S tried in refinement cycles gave the following result:

$$\begin{array}{l} \text{Cu}^{++}_3 \text{V}^{++}_4 \text{S}_4^{--} \quad \underline{R} \text{ unweighted} = 11.0\%, \quad \underline{R} \text{ weighted} = 5.8\% \\ \text{Cu}^+_3 \text{V}^{++++}_4 \text{S}_4^{--} \quad \underline{R} \text{ unweighted} = 11.1\%, \quad \underline{R} \text{ weighted} = 5.9\% \end{array}$$

In both cases the residuals became worse, suggesting that all the atoms in the structure are close to electroneutrality, a conclusion in harmony with a recent publication by L. Pauling (1965) in which the nature of the chemical bonds in sylvanite was discussed.

Closer agreement between the  $\underline{F}_{\text{obs}}$  and  $\underline{F}_{\text{calc}}$  was obtained by introducing anisotropic thermal parameters  $\beta_{ij}$ . Expressing the anisotropic temperature factor for atoms in special positions requires the determination of restrictions among the  $\beta_{ij}$ 's. These are discussed by H. A. Levy (1956). He states that the behavior of the  $\beta_{ij}$  can be

determined by examining the transformation of the products  $\underline{x}_i \underline{x}_j$ . The  $\underline{x}_i$ 's or, as the case may be, the  $\underline{x}_j$ 's with  $i, j = 1, 3$ , here stands for the coordinates  $\underline{x} \underline{y} \underline{z}$  of the particular atom to be considered. An example is shown in Table 3 with the atoms of sylvanite, all on sites with special symmetry. Hence the  $\beta_{ij}$  must be invariant to the transformation of  $\underline{x}_i \underline{x}_j$ ; H. A. Levy, (1956). When these properties of the  $\beta_{ij}$ 's were used, a few cycles of refinement led to the final  $\underline{R} = 9.8\%$  (unweighted) and  $\underline{R} = 5.2\%$  (weighted). The difference between these two residual values can be explained by a plot of  $\underline{R}$  versus  $\underline{F}_{obs}$  (see Fig. 6). This shows that the agreement between the  $\underline{F}_{obs}$  and  $\underline{F}_{calc}$  for weak intensities is a rather poor one, partly due to the unfavorable counting statistics for weak reflections. The final  $\underline{F}_{obs}$  and  $\underline{F}_{calc}$  are listed in Table 4.



Table 3

Computation of restrictions on the  $\beta_{ij}$ .

Cu, equipoint symmetry  $\bar{4}2\bar{m}$ .

Only the restriction of  $\bar{4}$  has to be considered since the others caused by 2 and  $\bar{m}$  are already implied in  $\bar{4}$ .  $xyz$  transforms to  $xz\bar{y}$  by  $\bar{4}$  axis.

ij	$x_i x_j$	$x'_i x'_j$	$\beta_{ij}$	
11	$x^2$	$x^2$	$\beta_{11} = \beta_{11}$	
22	$y^2$	$z^2$	$\beta_{22} = \beta_{33}$	
33	$z^2$	$y^2$	$\beta_{33} = \beta_{22}$	$\beta_{11}, \beta_{22}, \beta_{12} = \beta_{13} = \beta_{23} = 0$
12	$xy$	$xz$	$\beta_{12} = \beta_{13}$	
23	$yz$	$-yz$	$\beta_{23} = -\beta_{23}$	
31	$zx$	$-xy$	$\beta_{13} = -\beta_{12}$	

S, equipoint symmetry  $3\bar{m}$ .

The 3-fold axis imposes all the necessary restrictions including those caused by  $\bar{m}$ .  $xyz$  transforms to  $zxy$  by 3-fold axis.

ij	$x_i x_j$	$x'_i x'_j$	$\beta_{ij}$	
11	$x^2$	$z^2$	$\beta_{11} = \beta_{33}$	
22	$y^2$	$x^2$	$\beta_{22} = \beta_{11}$	
33	$z^2$	$y^2$	$\beta_{33} = \beta_{22}$	$\beta_{11} = \beta_{22} = \beta_{33}, \beta_{12} = \beta_{23} = \beta_{13}$
12	$xy$	$zx$	$\beta_{12} = \beta_{13}$	
23	$yz$	$xy$	$\beta_{23} = \beta_{12}$	
31	$zx$	$zy$	$\beta_{13} = \beta_{23}$	

V, equipoint symmetry  $\bar{4}3\bar{m}$ .

The combined restrictions of  $\bar{4}$  and 3 result in  $\beta_{11} = \beta_{22} = \beta_{33}$  and  $\beta_{12} = \beta_{13} = \beta_{23} = 0$ , thus causing a degeneration of the tensor-ellipsoid to a sphere.

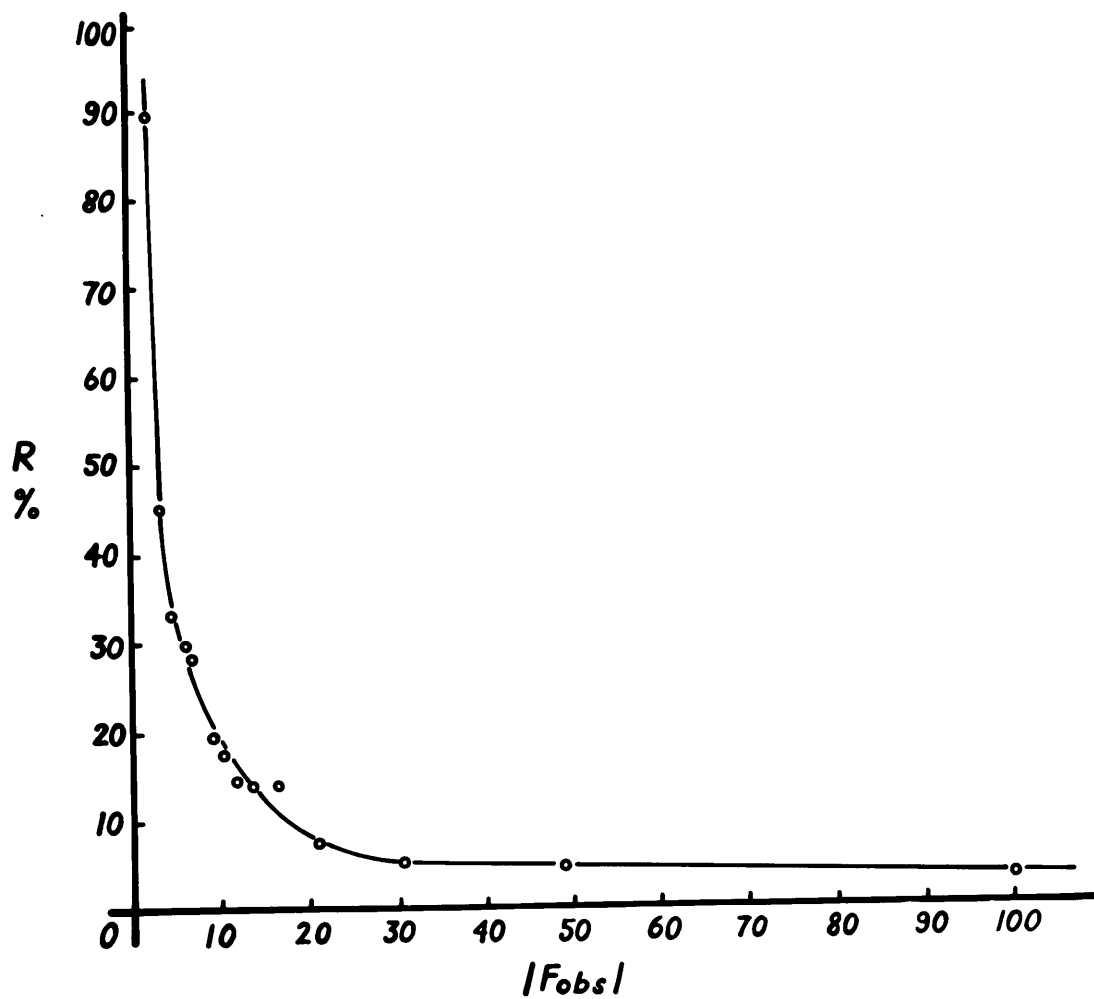


Fig. 6 Variation of the  $\underline{R}$  value in respect to  $\underline{F}_{obs}$ .

Table 4  
Final  $F_{\text{obs}}$  and  $F_{\text{calc}}$  of sulvanite.

h	k	l	$F_{\text{obs}}$	$F_{\text{calc}}$	h	k	l	$F_{\text{obs}}$	$F_{\text{calc}}$
2	0	0	83.66	78.23	4	3	0	27.06	28.61
3	0	0	47.38	44.13	5	3	0	9.43	8.00
4	0	0	153.59	152.02	6	3	0	31.67	31.67
5	0	0	57.20	52.02	8	3	0	11.83	15.38
6	0	0	34.11	29.28	10	3	0	12.95	13.88
7	0	0	10.89	5.64	11	3	0	5.27	4.24
8	0	0	58.43	54.28	12	3	0	11.83	8.69
9	0	0	27.40	23.81	14	3	0	7.71	5.94
10	0	0	13.50	14.08	4	4	0	99.33	101.46
11	0	0	5.93	1.34	5	4	0	34.87	37.42
12	0	0	18.59	17.66	6	4	0	21.97	21.19
13	0	0	5.85	8.99	7	4	0	6.88	6.56
14	0	0	7.04	7.18	8	4	0	41.97	42.38
1	1	0	13.95	11.14	9	4	0	16.73	18.95
2	1	0	69.30	65.65	10	4	0	11.61	12.04
3	1	0	10.82	10.75	12	4	0	14.68	14.86
4	1	0	48.83	51.62	13	4	0	4.03	7.59
5	1	0	6.69	2.57	5	5	0	1.73	5.59
6	1	0	30.06	28.57	6	5	0	7.66	12.56
8	1	0	22.60	21.48	8	5	0	17.97	18.25
9	1	0	6.60	2.57	11	5	0	6.02	.08
10	1	0	12.72	13.74	12	5	0	7.50	7.95
11	1	0	8.24	1.47	6	6	0	50.06	48.06
12	1	0	5.34	9.80	7	6	0	20.15	20.65
13	1	0	6.59	2.64	8	6	0	13.27	13.07
3	2	0	63.97	64.95	10	6	0	18.44	19.95
4	2	0	44.40	46.11	11	6	0	6.51	9.79
5	2	0	13.68	16.93	12	6	0	5.18	7.44
6	2	0	85.14	85.25	7	7	0	2.31	7.13
7	2	0	31.12	33.43	10	7	0	10.81	9.75
8	2	0	15.00	17.72	11	7	0	6.17	4.88
10	2	0	29.14	29.52	12	7	0	5.30	5.66
11	2	0	10.88	14.18	8	8	0	22.26	22.08
12	2	0	7.22	10.01	9	8	0	11.61	10.61
14	2	0	8.03	9.52	9	9	0	7.70	5.43
3	3	0	2.47	2.19	10	10	0	8.81	10.01

(Table 4, cont.)

h	k	l	F <sub>obs</sub>	F <sub>calc</sub>
1	1	1	130.33	134.71
2	1	1	15.83	15.29
3	1	1	95.28	92.55
4	1	1	16.40	15.69
5	1	1	54.67	56.73
6	1	1	15.43	15.78
7	1	1	34.31	31.62
8	1	1	12.89	13.63
9	1	1	16.22	15.52
10	1	1	12.68	10.23
11	1	1	7.48	6.58
2	2	1	67.86	66.51
3	2	1	11.54	9.55
4	2	1	39.96	40.05
5	2	1	8.55	7.19
6	2	1	30.23	30.79
7	2	1	7.55	3.29
8	2	1	17.14	18.70
10	2	1	16.38	14.07
11	2	1	5.31	3.04
13	2	1	3.65	1.94
14	2	1	6.59	6.26
3	3	1	68.84	70.72
4	3	1	12.23	12.90
5	3	1	48.76	46.91
6	3	1	14.56	13.36
7	3	1	26.31	26.11
9	3	1	14.73	13.45
10	3	1	8.65	9.09
11	3	1	4.27	5.53
12	3	1	5.17	6.71
14	3	1	5.35	4.78
4	4	1	38.85	35.93
5	4	1	9.81	8.62
6	4	1	21.30	22.97
7	4	1	6.03	4.74

h	k	l	F <sub>obs</sub>	F <sub>calc</sub>
8	4	1	17.89	18.40
9	4	1	7.63	3.97
10	4	1	9.94	12.19
12	4	1	10.68	8.70
5	5	1	32.18	31.25
6	5	1	9.85	9.23
7	5	1	22.30	19.24
8	5	1	9.92	8.90
9	5	1	8.56	9.36
10	5	1	6.30	7.12
11	5	1	5.77	4.37
12	7	2	4.75	6.27
8	8	2	10.97	10.13
9	8	2	4.80	5.16
10	8	2	14.88	13.96
11	8	2	7.24	7.06
9	9	2	5.07	.09
10	9	2	7.23	7.09
10	10	2	5.41	5.81
3	3	3	60.63	58.06
4	3	3	12.18	10.51
5	3	3	35.32	37.22
6	3	3	10.22	10.89
7	3	3	24.86	23.24
8	3	3	11.28	10.40
9	3	3	11.04	10.70
10	3	3	8.60	7.94
12	3	3	7.88	6.11
4	4	3	20.91	21.78
5	4	3	12.30	7.50
6	4	3	25.86	25.17
7	4	3	4.72	6.44
8	4	3	12.23	13.86
9	4	3	4.71	1.85
10	4	3	14.28	12.14
11	4	3	8.88	4.12

(Table 4, cont.)

h	k	l	F <sub>obs</sub>	F <sub>calc</sub>
5	5	3	29.69	28.05
6	5	3	10.87	9.09
7	5	3	13.90	15.12
8	5	3	10.39	7.20
9	5	3	12.63	8.96
10	5	3	4.87	6.73
12	5	3	4.50	5.16
13	5	3	5.38	1.58
7	6	3	5.26	4.57
8	6	3	13.64	14.57
9	6	3	4.70	5.06
10	6	3	7.92	9.16
11	6	3	7.67	2.16
12	6	3	8.54	7.03
7	7	3	12.12	10.75
8	7	3	6.91	6.20
9	7	3	3.68	4.95
11	7	3	3.87	2.68
12	7	3	4.92	4.14
8	8	3	9.88	9.72
9	8	3	8.24	3.42
10	8	3	10.52	8.18
11	8	3	6.85	3.53
4	4	4	70.51	72.98
5	4	4	27.53	28.70
6	4	4	17.69	17.05
8	4	4	32.37	33.60
9	4	4	13.55	15.46
10	4	4	8.30	10.47
12	4	4	10.47	12.58
13	4	4	4.75	6.52
5	5	4	6.80	7.73
6	5	4	8.66	11.81
7	5	4	5.94	3.12
8	5	4	14.79	15.40
11	5	4	4.71	1.01
12	5	1	4.54	5.59

h	k	l	F <sub>obs</sub>	F <sub>calc</sub>
6	6	1	21.50	20.29
7	6	1	9.43	6.44
8	6	1	13.16	14.22
9	6	1	4.62	3.63
10	6	1	10.60	10.88
11	6	1	5.69	3.40
12	6	1	4.16	7.34
13	6	1	3.65	2.30
7	7	1	13.58	11.17
8	7	1	4.73	5.82
9	7	1	6.87	6.32
10	7	1	5.42	5.46
12	7	1	4.19	4.42
8	8	1	14.22	11.76
10	8	1	7.74	8.36
11	8	1	2.93	2.99
9	9	1	3.24	3.41
10	10	1	6.59	6.46
2	2	2	60.66	61.08
3	2	2	33.26	34.82
4	2	2	117.90	122.43
5	2	2	40.47	43.76
6	2	2	23.85	24.39
7	2	2	4.86	6.09
8	2	2	46.81	47.70
9	2	2	17.70	21.23
10	2	2	12.56	13.04
12	2	2	15.28	16.19
13	2	2	8.10	8.24
3	3	2	10.29	10.67
4	3	2	43.59	43.18
5	3	2	6.52	5.17
6	3	2	17.23	19.57
8	3	2	21.74	20.07
10	3	2	10.47	11.50
12	3	2	9.13	8.91
4	4	2	28.91	28.80

(Table 4, cont.)

h	k	l	F <sub>obs</sub>	F <sub>calc</sub>
5	4	2	11.22	14.02
6	4	2	62.76	62.93
7	4	2	24.88	25.93
8	4	2	14.36	15.15
10	4	2	23.29	24.13
11	4	2	11.36	11.76
12	4	2	5.20	8.58
6	5	2	25.23	25.30
7	5	2	8.25	6.84
8	5	2	8.97	10.95
10	5	2	14.06	11.68
12	5	2	9.15	7.05
6	6	2	17.65	15.80
8	6	2	30.44	30.09
9	6	2	14.54	13.97
10	6	2	6.64	9.79
11	6	2	5.36	3.23
12	6	2	11.37	11.60
8	7	2	14.61	13.84
10	7	2	10.08	6.80
11	7	2	5.47	.33
12	5	4	4.62	7.09
6	6	4	37.85	38.00
7	6	4	17.30	16.91
8	6	4	9.91	11.52
9	6	4	5.65	4.95
10	6	4	17.05	16.66
11	6	4	8.18	8.32
12	6	4	6.80	6.45
7	7	4	6.68	6.55
8	7	4	10.22	7.25
10	7	4	10.16	8.53
11	7	4	4.86	4.34
8	8	4	19.69	18.39
9	8	4	7.73	9.08
10	8	4	8.29	7.12

h	k	l	F <sub>obs</sub>	F <sub>calc</sub>
9	9	4	6.56	4.78
10	9	4	3.49	4.53
5	5	5	17.64	17.57
6	5	5	7.56	5.35
7	5	5	14.70	12.89
9	5	5	4.11	5.62
10	5	5	4.52	5.17
12	5	5	5.76	4.47
6	6	5	18.15	17.08
7	6	5	5.34	6.50
9	6	5	6.13	2.12
10	6	5	6.53	8.97
8	7	5	7.99	3.90
9	7	5	7.01	4.61
10	8	5	7.39	6.08
9	9	5	3.44	2.75
10	9	5	4.83	3.06
6	6	6	10.35	12.23
8	6	6	18.67	20.22
9	6	6	12.05	9.92
10	6	6	4.97	7.59
11	6	6	4.92	3.39
8	7	6	10.23	10.14
9	7	6	6.06	4.86
10	7	6	3.41	5.61
11	7	6	4.03	1.50
8	8	6	10.42	7.98
10	8	6	7.01	10.02
7	7	7	4.26	5.53
10	7	7	3.54	3.24
8	8	8	8.68	10.92

### Discussion of the structure

The refinement confirmed the atomic arrangement for sylvanite as reported by Pauling and Hultgren, and improved it by a small shift of the coordinates of the sulfur atom. The final atomic parameters are listed in Table 5; the interatomic distances in Table 6; and the bond angles in Table 7. The anisotropic temperature coefficients computed by the least-squares refinement are presented in Table 8.

Both V and Cu are tetrahedrally coordinated to S. The tetrahedron about V is regular with the angle S-V-S =  $109^{\circ} 28'$ , while that about Cu is somewhat distorted with S-Cu-S angles of  $103^{\circ} 51'$  and  $112^{\circ} 21'$ . The S atom is surrounded by three Cu atoms situated at the middle of the cell edge, and by a V atom located at the origin; thus S has coordinating neighbors only on one side. The interatomic distances are similar to those reported for other structures. The Cu-S distance, 2.297 Å, is in agreement with values 2.28 Å listed by B. J. Wuensch and M. J. Buerger (1963) on chalcocite and 2.342 Å, 2.272 Å determined by B. J. Wuensch (1964) on tetrahedrite. The V-S distance, 2.214 Å, is about 0.1 Å shorter than V-S distances of 2.32 Å and 2.31 Å obtained by B. Pedersen and F. Grønvold (1959) on  $\alpha$  V<sub>3</sub>S and  $\beta$  V<sub>3</sub>S.

In order to study the possible thermal motion of the sulfur atom in its unusual coordination, a three-dimensional difference map was computed, based upon the structure refined with anisotropic thermal parameters. Two sections of this are shown in Fig. 7b and 7c, related to each other as illustrated in Fig. 7a. If the difference shown in Fig. 7b and 7c which represents about 1.2 electrons of the sulfur atom, can be regarded as significant, it appears that the sulfur atom cannot be represented by a spherical electron-density distribution modified by an elliptical thermal motion.

Table 5  
Final positional parameters and isotropic temperature factors of  
sulvanite

Atom	x	y	z	$\sigma(x)$	B
V	0.00	0.00	0.00		$0.3958 \text{ \AA}^2$
Cu	0.50	0.00	0.00		$1.2585 \text{ \AA}^2$
S	0.2372	0.2372	0.2372	0.0003	$1.0196 \text{ \AA}^2$

Table 6  
Interatomic distances in sulvanite

Atoms	Interatomic distances	$\sigma$
V-S	$2.214 \text{ \AA}$	$0.0009 \text{ \AA}$
Cu-S	$2.297 \text{ \AA}$	$0.001 \text{ \AA}$
V-Cu	$2.695 \text{ \AA}$	



Table 7

## Bond angles between atoms in sylvanite

Atoms	Bond angle	$\sigma$
S(xxx)-V(000)-S( $\bar{x}\bar{x}\bar{x}$ )	109° 28'	0.108°
S( $\bar{x}\bar{x}\bar{x}$ )-Cu( $\frac{1}{2}$ 00)-S( $\bar{x}\bar{x}\bar{x}$ )	103° 51'	0.044°
S(xxx)-Cu( $\frac{1}{2}$ 00)-S( $\bar{x}\bar{x}\bar{x}$ )	112° 21'	0.101°

Table 8

## Anisotropic temperature coefficients for the atoms in sylvanite

Atom	Symmetry	Symmetry restriction	$\beta$ values	$\sigma$
V	$\bar{4}3m$	$\beta_{11}=\beta_{22}=\beta_{33}$	$\beta_{11}=0.0036$	0.00026
		$\beta_{12}=\beta_{22}=\beta_{13}=0$		
Cu	$\bar{4}2m$	$\beta_{11}, \beta_{22}=\beta_{33}$	$\beta_{11}=0.0081$	0.00043
		$\beta_{12}=\beta_{23}=\beta_{13}=0$	$\beta_{22}=0.0122$	0.00035
S	3m	$\beta_{11}=\beta_{22}=\beta_{33}$	$\beta_{11}=0.0088$	0.00025
		$\beta_{12}=\beta_{23}=\beta_{13}$	$\beta_{12}=0.0018$	0.00051

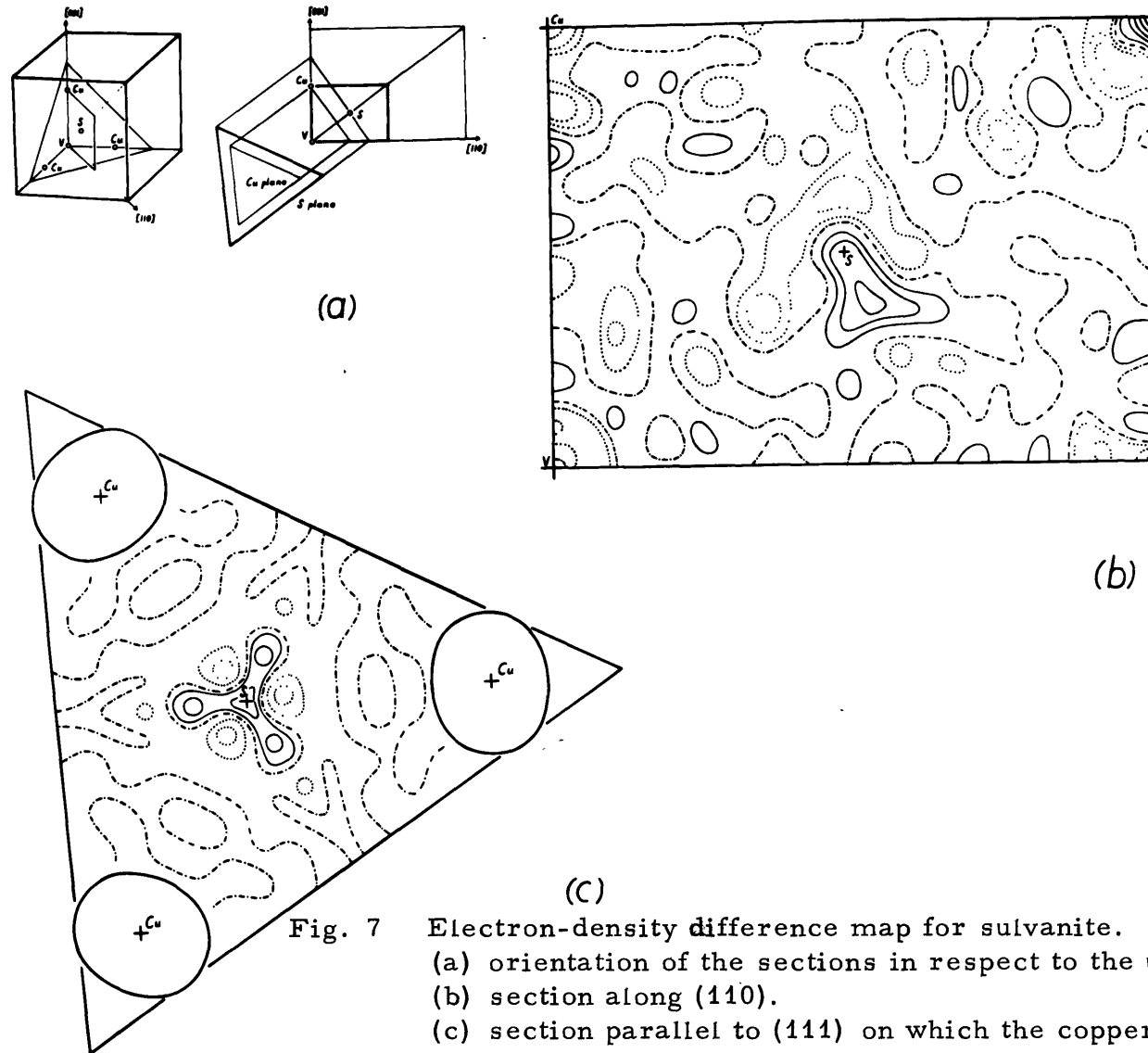


Fig. 7 Electron-density difference map for sylvanite.

- (a) orientation of the sections in respect to the unit cell.
- (b) section along (110).
- (c) section parallel to (111) on which the copper peaks from the density map are projected. Contours are at equal but arbitrary intervals, the negative contours are dotted, the zero contour is dash-dotted, and the positive contours are solid lines.

The maps may be interpreted as suggesting that there are thermal displacements directed into the empty space between pairs of the three nearest Cu neighbors. An attempt was made to split the S atom into three fractional atoms to approximate this kind of thermal vibration, but no improvement of the  $R$  factor resulted.

The V atom at the origin appears as a very sharp peak and has a low temperature factor. On the other hand, the peak representing Cu is smeared and of abnormally low height, suggesting a thermal motion, which, as the difference map shows, can be represented in this case by an ellipsoid. H. A. Levy (1956) gives a transformation formula which expresses the anisotropic temperature coefficients  $\beta_{ij}$  in terms of the components  $\rho_{ij}$  related to the crystal axes in direct space:

$$\beta_{ij} = 2\pi^2 \sum_{k=1}^3 \rho_k^i \rho_k^j .$$

The  $\rho_{ij}$  symbolize the root-mean-square thermal displacements. Due to the point-group symmetry of the Cu-site, the thermal ellipsoid has its principal axes parallel to the crystal axes. The magnitudes of the axes from the thermal ellipsoid were found to be  $\rho_{11} = 0.110 \text{ \AA}$ ,  $\rho_{22} = 0.134 \text{ \AA}$ , and  $\rho_{33} = 0.134 \text{ \AA}$ , thus indicating that the Cu atom has a higher thermal displacement perpendicular to the  $\bar{4}$  axis ( $\rho_{22}$  and  $\rho_{33}$ ) than parallel to it ( $\rho_{11}$ ).

### Appendix

For the general-radiation streak correction, two programs, MINTE 1 and MINTE 2, were written in FORTRAN II for the IBM 7094 computer of the M. I. T. Computation Center. The section of MINTE 1 which computes constants was taken over from the FINTE 2 program written by H. H. Onken (1964).

MINTE 1. This program calculates all possible lattice points which give rise to a general-radiation streak affecting other lattice points within a given wave-length range. The data deck for MINTE 1 consists of the output from FINTE 2, FORMAT (3I3, 2X, F6.2, X, F6.2, X, F6.4, X, F6.4, X, F9.2, 9X, F8.3). The program prepares two output decks, both in printed and punched form. The first deck lists a reflection  $\underline{hkl}$  and all the other reflections  $\underline{h' k' l'}$  on the same lattice row but with lower  $\sin \theta$  and their percentage  $\underline{R_{\lambda_i}}$  of  $\underline{I (h' k' l')}$  contributing to  $\underline{I (hkl)}$ , e. g. :

h	k	l	effected by	$\underline{R_{\lambda_i}}$	of	h'	k'	l'
9	0	0		0.088		8	0	0
9	0	0		0.041		7	0	0
9	0	0		0.013		6	0	0

The second output deck, again in printed and punched form, gives the reflections which either affect other ones, or are affected by other reflections.

In the present write-up MINTE 1 can handle white-radiation streaks within a  $\lambda$ -range of  $0.5 \overset{\circ}{\text{Å}}$  up to  $3.15 \overset{\circ}{\text{Å}}$ . The spectral distribution can be obtained by examining a lattice line with a strong reflection at the lowest possible  $\theta$ , which therefore is not affected by other radiation streaks.

## Set-up for MINTE 1

Request card: Tape A5 scratch.

\* XEQ

MINTE 1

\* DATA

TITLE any character in col. 1-72.

SENSE CARD col. 1 ISET = 1 rotation axis is c.  
 2 rotation axis is b.  
 3 rotation axis is a.

CELL CARD	col. 1-7	a*	FORMAT (7F7.4) the same as used in FINTE 2.
	col. 8-14	b*	
	col. 15-21	c*	
	col. 22-28	$\alpha$ *	
	col. 29-35	$\beta$ *	
	col. 36-42	$\gamma$ *	
	col. 43-49	$\lambda$	

## LAMBDA CARDS

## FORMAT (18 F 4.3)

<u>First card</u>			<u>Second card</u>			<u>Third card</u>		
F4.3	$\lambda$	$R_\lambda$	F4.3	$\lambda$	$R_\lambda$	F4.3	$\lambda$	$R_\lambda$
1	0.50	--	19	1.40	--	37	2.30	--
2	0.55	--	20	1.45	--	38	2.35	--
3	0.60	--	21	1.50	--	39	2.40	--
4	0.65	--	22	1.55	--	40	2.45	--
5	0.70	--	23	1.60	--	41	2.50	--
6	0.75	--	24	1.65	--	42	2.55	--
7	0.80	--	25	1.70	--	43	2.60	--
8	0.85	--	26	1.75	--	44	2.65	--
9	0.90	--	27	1.80	--	45	2.70	--
10	0.95	--	28	1.85	--	46	2.75	--
11	1.00	--	29	1.90	--	47	2.80	--
12	1.05	--	30	1.95	--	48	2.85	--
13	1.10	--	31	2.00	--	49	2.90	--
14	1.15	--	32	2.05	--	50	2.95	--
15	1.20	--	33	2.10	--	51	3.00	--
16	1.25	--	34	2.15	--	52	3.05	--
17	1.30	--	35	2.20	--	53	3.10	--
18	1.35	--	36	2.25	--	54	3.15	--

REFLECTION DECK FINTE 2 output

END CARD 1 in col. 72

```

*M4187-3689,FMS,RESULT,5MIN,5MIN,5000LINES,5000CARDS
*   XEQ
*   LIST
*   LABEL
CMINTE1
C   PROGRAM FOR COMPUTING INTENSITIES CORRECTED FOR
C   GENERAL RADIATION STREAKS ALONG LATTICE LINES
    DIMENSION TITLE(15),S(54),IH(1000),IK(1000),IL(1000)
  100 READ INPUT TAPE 4,101,TITLE
  101 FORMAT(15A5)
    READ INPUT TAPE 4,102,ISET
  102 FORMAT(I1)
    READ INPUT TAPE 4,103,A,B,C,AL,BE,GA,WV
  103 FORMAT(7F7.4)
    READ INPUT TAPE 4,110,(S(JJ),JJ=1,54)
  110 FORMAT(18F4.3)
    J=0
    III=0
    IND=1
    WRITE OUTPUT TAPE 2,104,TITLE
  104 FORMAT (1H115A5)
C                                     COMPUTE CONSTANTS
  200 PI=3.1415927
    PIH=PI/2.0
    RAD=PI/180.0
    GO TO (201,202,203),ISET
  201 AP=A*WV
    BP=B*WV
    CP=C*WV
    ALP=AL*RAD
    BEP=BE*RAD
    GAP=GA*RAD
    GO TO 204
  202 AP=C*WV
    BP=A*WV
    CP=B*WV
    ALP=GA*RAD
    BEP=AL*RAD
    GAP=BE*RAD
    GO TO 204
  203 AP=B*WV
    BP=C*WV
    CP=A*WV
    ALP=BE*RAD
    BEP=GA*RAD
    GAP=AL*RAD
  204 A=AP
    B=BP
    C=CP
    AL=ALP
    BE=BEP
    GA=GAP
    CAL=COSF(AL)
    CBE=COSF(BE)
    CGA=COSF(GA)

```

```

SGA=SINF(GA)
ABG=A*B*CGA
BCA=B*C*CAL
CAB=C*A*CBE
AA=A*A
BB=B*B
CC=C*C
REWIND 9
300 CONTINUE
READ INPUT TAPE 4,301,MH,MK,ML,UPS,PHI,VLP,STH,FINTE,COFAK,LAST
301 FORMAT(3I3,2X,F6.2,1X,F6.2,1X,F6.4,1X,F6.4,1X,F9.2,9X,F8.3,6X,I1)
888 IF(LAST)800,800,904
800 NH=XABSF(MH)
    NK=XABSF(MK)
    NL=XABSF(ML)
    NSUM=NH+NK+NL
    NSU=NSUM
862 NSU=NSU-1
    IF(NSU)864,864,851
851 JH=(NH*NSU)/NSUM
    JK=(NK*NSU)/NSUM
    JL=(NL*NSU)/NSUM
    JSU=JH+JK+JL
    IF(JSU)864,864,853
853 SSUM=JSU
    SH=NH
    SK=NK
    SL=NL
    SNU=NSU
    SUMN=NSUM
    SH=SH*SNU/SUMN
    SK=SK*SNU/SUMN
    SL=SL*SNU/SUMN
    SUMJ=SH+SK+SL
    ST=SUMN/SSUM
    SJ=SUMN/SUMJ
    IF(ST-SJ)852,852,862
852 IHH=(JH*MH)/NH
    KK=(JK*MK)/NK
    LL=(JL*ML)/NL
    GO TO(855,856,857),ISET
855 TTH=IHH
    TTK=KK
    TTL=LL
    GO TO 858
856 TTH=LL
    TTK=IHH
    TTL=KK
    GO TO 858
857 TTH=KK
    TTK=LL
    TTL=IHH
858 TTLC=TTL*TTL*CC
    SSIG=TTH*TTH*AA+TTK*TTK*BB+2.0(TTH*TTK*ABG+TTK*TTL*BCA+TTL*TTH*CAB
1)

```



```

      STHH=SQRTF(SSIG+TTLC)/2.0
C     CALCULATION OF LAMBDA=2D*SIN(THETA)
      DD=WV/STHH
      WW=DD*STH
      SR=WW/0.05-9.0
      M=XINTF(SR)
      W=INTF(SR)
      RT=(SR-W)*(S(M+1)-S(M))+S(M)
      IF(RT-0.005)864,864,859
859   I=J+1
      IH(I)=IHH
      IK(I)=KK
      IL(I)=LL
      J=I
      WRITE OUTPUT TAPE 2,860,MH,MK,ML,RT,IHH,KK,LL
860   FORMAT(3I3,2X,12H EFFECTED BY,X,F4.3,X,2HOF,X,3I3)
      WRITE OUTPUT TAPE 3,861,MH,MK,ML,IHH,KK,LL,RT
861   FORMAT(3I3,2X,3I3,2X,F4.2)
      III=1
      GO TO 862
864   II=III
      III=0
      IF(II)929,929,927
927   WRITE TAPE 9,MH,MK,ML,UPS,PHI,VLP,STH,FINTE,COFAK,IND,LAST
      GO TO 300
929   IND=0
      WRITE TAPE 9,MH,MK,ML,UPS,PHI,VLP,STH,FINTE,COFAK,IND,LAST
      IND=1
      GO TO 300
904   CONTINUE
      IND=0
      WRITE TAPE 9,MH,MK,ML,UPS,PHI,VLP,STH,FINTE,COFAK,IND,LAST
      REWIND 9
206   NORD=0
      WRITE OUTPUT TAPE 2,207
207   FORMAT( 78H1  H    K    L    UPS    PHI    1/LP    SIN
1     INTENSITY  DEVIATION)
333   READ TAPE 9,MH,MK,ML,UPS,PHI,VLP,STH,FINTE,COFAK,IND,LAST
      IF(LAST)931,931,920
931   IF(IND-1)909,908,909
909   DO 910 JI=1,I
      IF(MH-IH(JI))910,906,910
906   IF(MK-IK(JI))910,907,910
907   IF(ML-IL(JI))910,908,910
910   CONTINUE
      GO TO 333
908   WRITE OUTPUT TAPE 2,922,MH,MK,ML,UPS,PHI,VLP,STH,FINTE,COFAK
922   FORMAT(3(2X,I3),2(F10.2),2(F10.4),F12.2,F12.3)
      WRITE OUTPUT TAPE 3,928,MH,MK,ML,UPS,PHI,VLP,STH,FINTE,COFAK
928   FORMAT(3I3,2X,F6.2,1X,F6.2,1X,F6.4,1X,F6.4,1X,F9.2,9X,F8.3)
911   NORD=NORD+1
      IF(50-NORD)206,333,333
920   WRITE OUTPUT TAPE 2,921
921   FORMAT(11H END OF RUN)
      CALL EXIT

      END
*     DATA

```

MINTE 2. The original data deck has been reduced by MINTE 1 to reflections which are effected by a general radiation streak or to reflections which give rise to such a streak. The program performs the necessary corrections on the observed intensities according to the equation (A. C. Larson, 1965).

$$\text{corrected } I_{\underline{nH}} = I_{\underline{nH}} - \sum_{i=a}^{n-1} I_{\underline{iH}} \cdot R_{\lambda_i} \cdot \cos \theta_{\underline{nH}} \quad n > a$$

where  $I_{\underline{iH}}$  is the  $i$  th intensity affecting  $I_{\underline{nH}}$  by its white-radiation streak.  $R_{\lambda_i}$  is defined as the percentage of  $I_{\underline{iH}}$  contributing to  $I_{\underline{nH}}$ . The function  $\cos \theta_{\underline{nH}}$  was found to be a good approximation for the change of the effective window width. Following equivalent symbols were used in the program:

$$I_{\underline{iH}} = \text{FINITE (K)}$$

$$I_{\underline{nH}} = \text{FINITE (J)}$$

$$R_{\lambda_i} = \text{RT (MN)}$$

$$\cos \theta_{\underline{nH}} = \text{COTH}$$

MINTE 1 produces two output decks, which are used in MINTE 2 as the data deck, each with an end card. The final output of MINTE 2 is obtainable in FORMAT (3I3, 2X, F6.2, X, F6.2, X, F6.4, X, F6.4, X, F9.2, 9X, F8.3) and is thus suitable for further processing with the GAMP program.

**Set-up for MINTE 2**

- \* XEQ  
MINTE 2
- \* DATA  
TITLE any character in col. 1-72.  
MINTE 1 OUTPUT I  
END CARD 1 in col. 72.  
MINTE 1 OUTPUT II  
END CARD 1 in col. 72.

```

*M4187-3689,FMS,RESULT,5MIN,5MIN,5000LINES,5000CARDS
*   XEQ
*   LIST
*   LABEL
CMINTE2
C   PROGRAM CORRECTS INTENSITIES WHICH ARE EFFECTED BY
C   GENERAL RADIATION STREAKS ALONG LATTICE LINES , DATA DECK
C   SORTED WITH INCREASING SIN(THETA).
   DIMENSION TITLE(15),MH(400),MK(400),ML(400),UPS(400),PHI(400)
   DIMENSION VLP(400),STH(400),FINTE(400),COFAK(400),NH(600),NK(600)
   DIMENSION NL(600),NNH(600),NNK(600),NNL(600),RT(600),MMH(400)
   DIMENSION MMK(400),MML(400)
   READ INPUT TAPE 4,1,TITLE
001  FORMAT(15A5)
      DO 2 I=1,600
        READ INPUT TAPE 4,3,NH(I),NK(I),NL(I),NNH(I),NNK(I),NNL(I),RT(I),
1LAST
003  FORMAT(3I3,2X,3I3,2X,F4.2,45X,I1)
      II=I
      IF(LAST)2,2,4
002  CONTINUE
004  DO 5 J=1,400
      READ INPUT TAPE 4,6,MH(J),MK(J),ML(J),UPS(J),PHI(J),VLP(J),STH(J),
1FINTE(J),COFAK(J),LAST
006  FORMAT(3I3,2X,F6.2,1X,F6.2,1X,F6.4,1X,F6.4,1X,F9.2,9X,F8.3,6X,I1)
      JJ=J
      MMH(J)=MH(J)
      MMK(J)=MK(J)
      MML(J)=ML(J)
      IF(LAST)5,5,7
005  CONTINUE
007  WRITE OUTPUT TAPE 2,113,TITLE
113  FORMAT(1H115A5)
      WRITE OUTPUT TAPE 2,101
101  FORMAT(50H  H   K   L   EFFECTED BY   FINTE   CORRECTION)
      M=JJ-1
      DO 110 KJ=1,M
        JK=KJ+1
        DO 110 NJ=JK,JJ
          IF(STH(KJ)-STH(NJ))110,110,109
109  S=STH(KJ)
      T=STH(NJ)
      STH(KJ)=T
      STH(NJ)=S
      JHA=MH(KJ)
      JHB=MH(NJ)
      MH(KJ)=JHB
      MH(NJ)=JHA
      JKA=MK(KJ)
      JKB=MK(NJ)
      MK(KJ)=JKB
      MK(NJ)=JKA
      JLA=ML(KJ)
      JLB=ML(NJ)
      ML(KJ)=JLB

```

```

ML(NJ)=JLA
FS=FINTE(KJ)
FT=FINTE(NJ)
FINTE(KJ)=FT
FINTE(NJ)=FS
DS=COFAK(KJ)
DT=COFAK(NJ)
COFAK(KJ)=DT
COFAK(NJ)=DS
TUPS=UPS(KJ)
FUPS=UPS(NJ)
UPS(KJ)=FUPS
UPS(NJ)=TUPS
TPHI=PHI(KJ)
FPHI=PHI(NJ)
PHI(KJ)=FPHI
PHI(NJ)=TPHI
TVLP=VLP(KJ)
FVLP=VLP(NJ)
VLP(KJ)=FVLP
VLP(NJ)=TVLP
110 CONTINUE
DO 100 J=1,JJ
III=II+1
DO 19 I=1,II
MN=III-I
IF(MH(J)-NH(MN))19,8,19
008 IF(MK(J)-NK(MN))19,10,19
010 IF(ML(J)-NL(MN))19,11,19
011 DO 20 K=1,JJ
IF(NNH(MN)-MH(K))20,15,20
015 IF(NNK(MN)-MK(K))20,16,20
016 IF(NNL(MN)-ML(K))20,17,20
017 COTH=COSF(ASINF(STH(J)))
FINT=FINTE(K)*RT(MN)*COTH
WRITE OUTPUT TAPE 2,18,MH(J),MK(J),ML(J),NNH(MN),NNK(MN),NNL(MN),
1FINTE(J),FINT
018 FORMAT(3(I3,X),2X,3(I3,X),2X,F9.2,2X,F9.2)
FINTE(J)=FINTE(J)-FINT
IF(FINTE(J))208,19,19
208 FINTE(J)=0.0
GO TO 19
020 CONTINUE
019 CONTINUE
100 CONTINUE
WRITE OUTPUT TAPE 2,207
207 FORMAT(78H1 H K L UPS PHI 1/LP SIN
1 FINTECORR DEVIATION)
DO 102 K=1,JJ
DO 209 L=1,JJ
IF(MMH(K)-MH(L))209,210,209
210 IF(MMK(K)-MK(L))209,211,209
211 IF(MML(K)-ML(L))209,212,209
212 WRITE OUTPUT TAPE 2,103,MH(L),MK(L),ML(L),UPS(L),PHI(L),VLP(L),
1STH(L),FINTE(L),COFAK(L)

```

```
103  FORMAT(3(2X,I3),2(F10.2),2(F10.4),F12.2,F12.3)
      WRITE OUTPUT TAPE 3,108,MH(L),MK(L),ML(L),UPS(L),PHI(L),VLP(L),
108  1STH(L),FINTE(L),COFAK(L)
      FORMAT(3I3,2X,F6.2,1X,F6.2,1X,F6.4,1X,F6.4,1X,F9.2,9X,F8.3)
      GO TO 102
209  CONTINUE
102  CONTINUE
      WRITE OUTPUT TAPE 2,104
104  FORMAT(11H END OF RUN)
      CALL EXIT
      END
*    DATA
```

### Acknowledgements

The author is grateful to Professor Buerger for suggesting and supervising this thesis and thanks him for his continued interest. He also expresses thanks to Mr. Wayne A. Dollase for many discussions which contributed to this work. The writer would like to acknowledge the help of Mr. William Blackburn who kindly provided a spectroscopic analysis of sylvanite crystals. The computations were carried out on the IBM 7094 computer at the Massachusetts Institute of Technology Computation Center. This work was supported by a grant from the National Science Foundation.

References

- Berry, L. G. and Thompson, R. M. (1962). X-ray powder data for ore minerals: the Peacock Atlas. p. 57. The Geological Society of America, New York.
- DeJong, W. F. (1928). Struktur des Sulvanit,  $\text{Cu}_3\text{VS}_4$ . Z. Kristallogr. 68, 522-529.
- De Vries, A. On weights for a least-squares refinement. Acta Cryst. 18, (1965) 1077.
- Kartha, G. and Ahmed, F. R. Structure-factor calculation with anisotropic thermal parameters. Acta Cryst. 13, (1960) 532-534.
- Larsen, A. C. A three-dimensional refinement. Acta Cryst. 18, (1965) 717-724.
- Levy, H. A. Symmetry relations among coefficients of the anisotropic temperature factor. Acta Cryst. 9, (1956) 679.
- Lundquist, D. and Westgren, A. The crystal structure of  $\text{Cu}_3\text{VS}_4$ . Svenk. Kem. Tidskr. 48, (1936) 241-243.
- Onken, H. H. Manual for some computer programs for x-ray analysis. (1964) Cambridge, Massachusetts Institute of Technology.
- Pauling, L. and Hultgren, R. The crystal structure of sulvanite,  $\text{Cu}_3\text{VS}_4$ . Z. Kristallogr. 84, (1933) 204-212.
- Pauling, L. The nature of the chemical bonds in sulvanite,  $\text{Cu}_3\text{VS}_4$ . Tschermaks Min. Petr. Mitt. (3 Folge) 1-6, (1965) 379-384.
- Pedersen, B. and Grønvold, F. The crystal structures of  $\alpha\text{-V}_3\text{S}$  and  $\beta\text{-V}_3\text{S}$ . Acta Cryst. 12, (1959) 1022-1027.



- Philips Electronic Instruments, Mount Vernon, New York. Norelco  
Radiation Detectors Instruction Manual.
- Trueblood, K. N. Symmetry transformation of general anisotropic  
temperature factors. *Acta Cryst.* 9, (1956) 359-361.
- Willis, B. T. M. The anomalous behavior of the neutron reflexions of  
fluorite. *Acta Cryst.* 18, (1965) 75-76.
- Wuensch, B. J. and Buerger, M. J. The crystal structure of chalcocite,  
 $\text{Cu}_2\text{S}$ . Mineralogical Society of America, (1963) Special Paper 1.
- Wuensch, B. J. The crystal structure of tetrahedrite,  $\text{Cu}_{12}\text{Sb}_4\text{S}_{13}$ .  
*Z. Kristallogr.* 119 (1964) 437-453.